DESIGN OF A SERVOMECHANISM FOR USE IN TAKING MICROWAVE ANTENNA PATTERN MEASUREMENTS

A Thesis

Presented to

the Faculty of Graduate Studies and Research

The University of Manitoba

In Partial Fulfillment

of the Requirements for the Degree

Master of Science

in

Electrical Engineering

by

William G. Stephens

September 1965

ABSTRACT

This thesis gives an account of the design and building of a feedback control system for the purpose of measuring microwave antenna patterns. The text begins with a statement of the problem thus establishing the essential characteristics of the control system. Next a preliminary investigation into existing equipment and a final system choice is made. The problems encountered with this system and their solution are discussed and finally the complete characteristics of the control system and its method of operation are given.

ACKNOWLEDGEMENTS

The author is indebted to Mr. W. H. Lehn (Professor, University of Manitoba) for his continued guidance throughout the project, to the University of Manitoba Research Fund (Grant No. E14-58(39)) for financial assistance, and to the technicians who helped in fabricating equipment for the project.

TABLE OF CONTENTS

LIST OF TABLES

LIST OF FIGURES

CHAPTER 1

AN INTRODUCTORY STATEMENT OF THE PROBLEM AND ITS IMPLICATIONS

Basically the problem was to design and build a servomechanism unit with which microwave antenna pattern measurements could be made. This was to be accomplished by employing existing control equipment at the University of Manitoba which was not in continuous use.

The microwave antenna pattern range consisted of a test antenna capable of rotating at 0 to 3 r.p.m. and a receiving horn as can be seen in Fig. 1a. The receiving horn contained a variable attenuator behind which was a crystal as shown in Fig. 1b. From the crystal the signal went to a voltage standing wave ratio meter (hereafter designated VSWR meter) where it was transformed into a D.C. voltage.

Since it is necessary that the crystal not exceed the range of square law operation, the variable attenuator must move in such a fashion that microwave signal strength does not surpass this range. Thus the servomechanism must move the attenuator to meet this requirement and by so doing its position is automatically a function of input microwave strength. A block diagram of the system appears in Fig. 2 where it can be seen that the output potentiometer, by being mechanically linked to the attenuator, will have a wiper voltage directly proportional to the attenuator position.

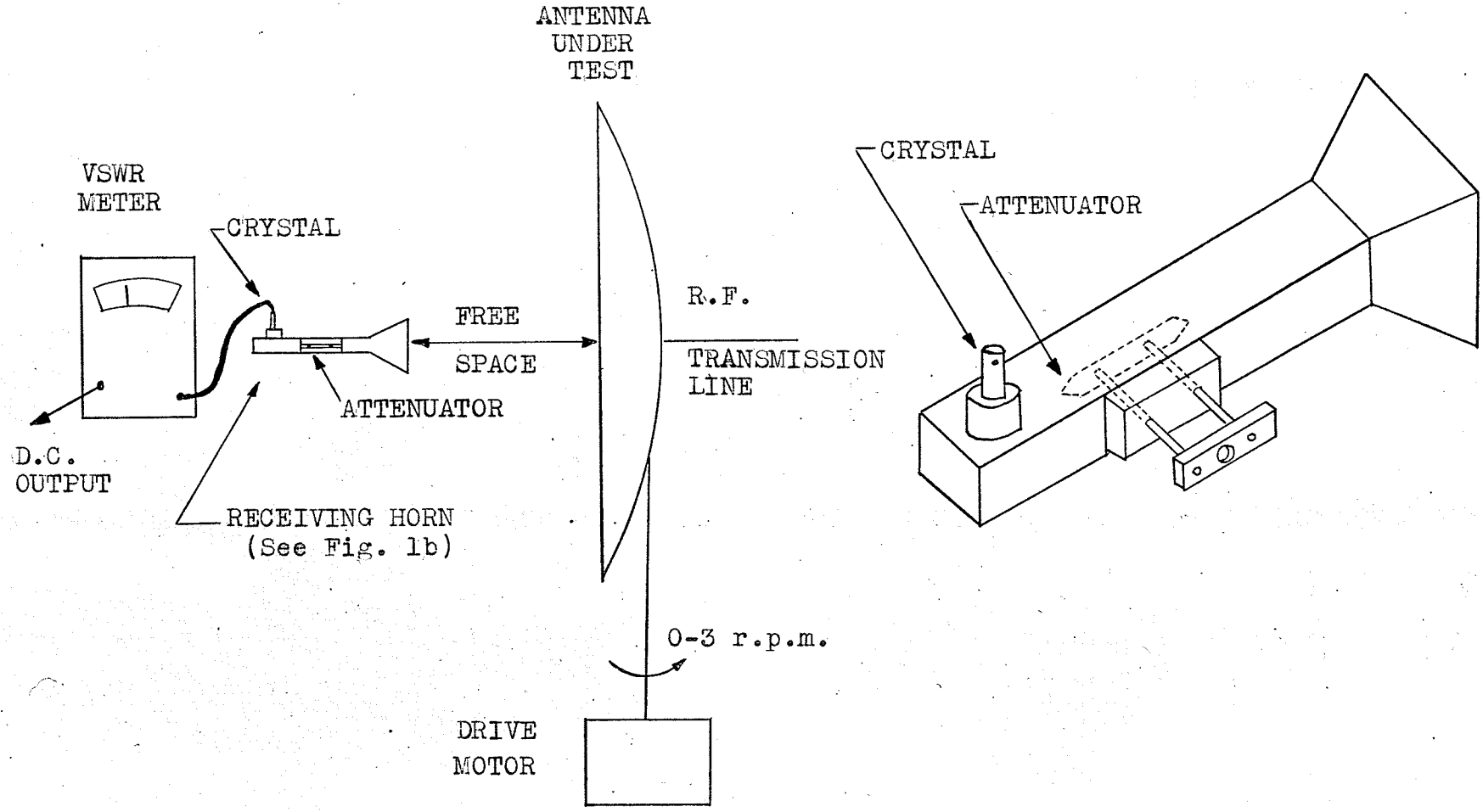

FIGURE 1 a) MICROWAVE ANTENNA PATTERN RANGE EQUIPMENT

b) INPUT HORN CONTAINING VARIABLE ATTENUATOR AND CRYSTAL

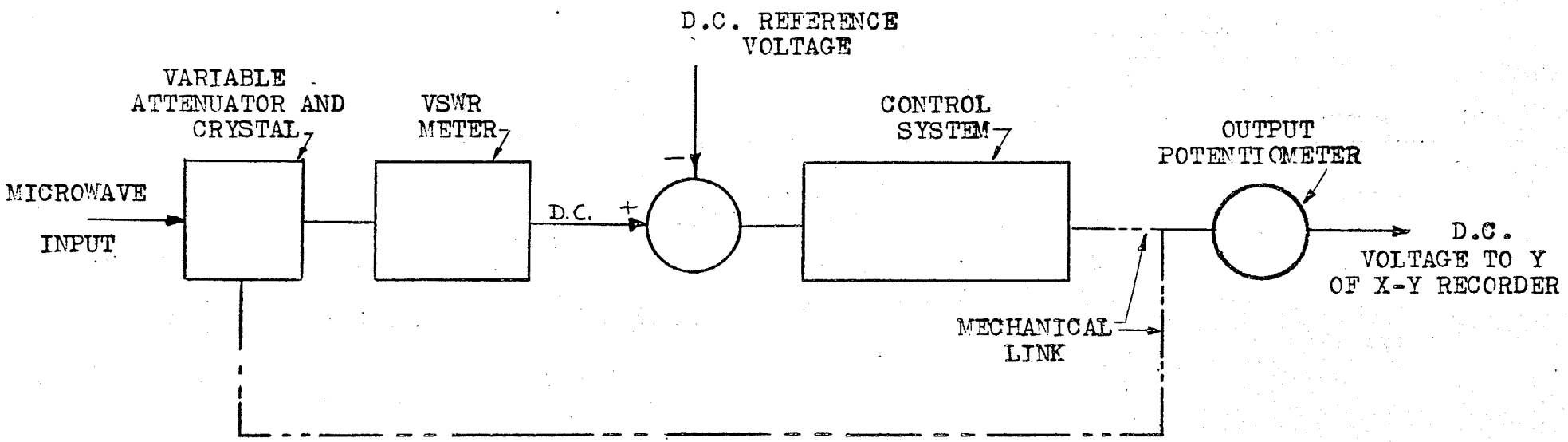

FIGURE 2 ANTENNA PATTERN MEASURING SYSTEM

The D. C. voltage from this potentiometer gives the Y reading on the X-Y recorder. At the same time the X reading is a direct function of the angular position of the transmitting antenna.

No rigid specifications were given for the control system to meet. It must, however, be capable of handling a 40 db. range with the least error and best response characteristics obtainable.

The main justification for building such a system is quite simply one of economy. To buy an antenna pattern analyzer to do the same job would mean an expense of two to three thousand dollars. The cost of the servomechanism unit, on the other hand, centers around the servomotor, gears, an amplifier, and the variable attenuator which may run to three hundred dollars. The remainder of the necessary equipment, the VSWR meter, D. C. amplifier, and equipment necessary for the 400 cycle supply, can all be used for various other purposes. Therefore this alternate procedure for taking antenna pattern measurements offers a considerable saving.

As well as being economical it is theoretically possible for this servo system to at least match the accuracy of a receiver type system which is in the order of 0.1 db. per 10 db. of dynamic range.[1] The only conceivable disadvantage would be a longer time required for one pattern measurment due to slower response time on the part of the servo system.

The following chapters consist, respectively, of preliminary investigations into available control equipment for the project, a study of the problems associated with the system eventually chosen,

attempts at compensation, and the final resulting system and its characteristics.

CHAPTER 2

PRELIMINARY INVESTIGATIONS INTO EXISTING EQUIPMENT AND FINAL SYSTEM CHOICE

Since the problem involved no rigid design specifications but rather that a system "that will be satisfactory" be constructed, the choice of the system could only be made on an assumptive basis.

The prime mover which has the most desirable dynamic characteristics and which also meets power requirements should be chosen, provided of course that it is backed by an adequate power supply and amplifier. The power required was an unknown but the load would consist of a reference potentiometer and a mechanism driving the attenuator. It was assumed that the attenuator drive mechanism would constitute a load of about the same magnitude as that of the potentiometer.

With this rough guess in mind, servo control unit #921B1, consisting of a D.C. input to a chopper amplifier to a 60 cycle Holtzer Cabot type RBC2505 servomotor, equipped with feedback, was tested. The test consisted of mounting the motor geared to a potentiometer on a breadboard, applying a specific step input and recording the output signal. The same test was used with a system consisting of a D.C. signal modulated to 400 cycles and fed to a Kearfott Co. Inc. type R-603-1A magnetic amplifier, which in turn drove a motor. Several motors were tested with this system and the best dynamic response was recorded with the 400 cycle Beckman Model 18SM491 servomotor.

Briefly then, the system chosen consisted of a 400 cycle power supply, modulator, magnetic amplifier and servomotor as can be seen in Fig. 3. Although inherent with this system were a considerable number of practical problems, which will be explained in the next chapter, it was felt that it would ultimately do the most satisfactory job and for this reason alone was selected.

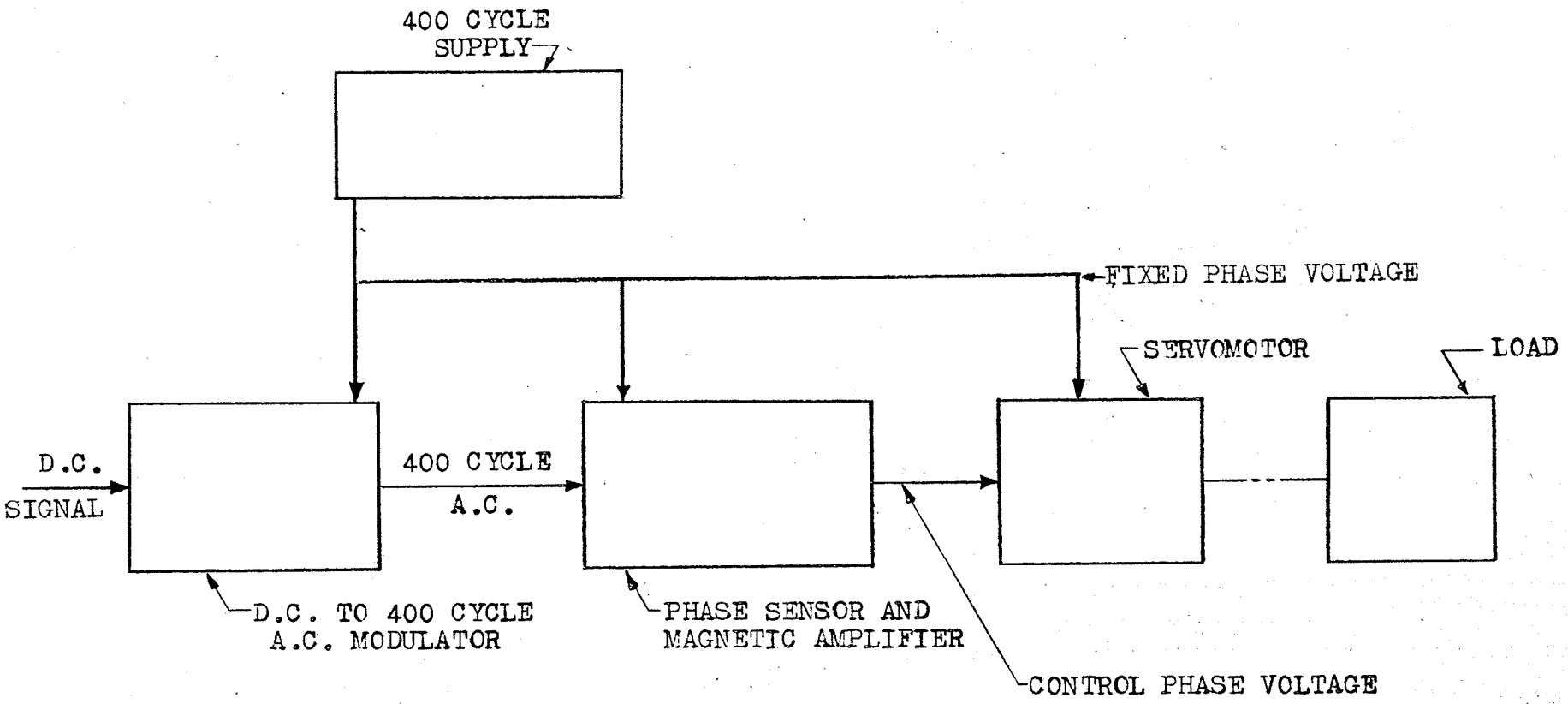

FIGURE 3 FINAL CONTROL SYSTEM CHOICE

CHAPTER 3

CONSTRUCTING THE SYSTEM

Many practical problems were encountered with the equipment in each control block. This chapter will deal with these problems as well as the problem of piecing all the blocks together to give a working system.

1. INDIVIDUAL BLOCK DIAGRAM PROBLEMS

The 400 cycle supply[2] (See Appendix A) available was a D.C. to A.C. parallel inverter employing silicon controlled rectifiers which was capable of producing about 19 watts, 115 volts r.m.s. at loads of 300 ohms to open circuit. The servomechanism was expected to draw about 18.5 watts. Thus overloading of the 400 cycle supply was not expected to be a problem, but in any case a thermal overload switch on the Lambda D.C. power supply driving the 400 cycle supply would prevent damage to the equipment should the load drop below 300 ohms.

Some difficulty was experienced in making this unit operate. Larger silicon controlled rectifiers were substituted and with appropriate adjustments of the Lambda Regulated Power Supply Model LA 50-03 AM and the Tektronix type 105 square wave generator, it functioned satisfactorily when droving all the required loads. Final operating values were 22 volts for the Lambda and maximum output for the Tektronix.

The output voltage waveshape of the 400 cycle supply as shown in Fig. 4 caused considerable consternation. The possibility of filtering was rejected since it would absorb too much power.

The only literature that could be found on the effects of non-sinusoidal excitation for servomotors[3] indicated that for square wave excitation on both reference and control phase, motor velocity and acceleration were similar in form but more oscillatory than for normal sinusoidal excitation. This waveform would then likely be satisfactory in driving the servomotor even though the motor would be noisy and heat more than normal. Thus it was assumed that this power supply would be adequate.

The D.C. to 400 cycle A.C. modulator chosen was of the form shown in Fig. 5. The A.C. output of this modulator is proportional in magnitude to the D.C. input and of a polarity depending upon the polarity of the D.C. input. Thus for a positive D.C. input, the output will be 180° out of phase with that for a corresponding negative D.C. input. The diodes were matched so that they all had similar characteristics and all resistors are within 10 ohms of each other. Care was taken in soldering resistors and diodes together so that their values would not change. Two alterations were required in this circuit which will be shown later.

The input to the Kearfott magnetic amplifier required the circuit suggested in the Kearfott Manual and shown in Fig. 6. The 5963 Tube is an "ON-OFF" control tube ideal for this purpose. Capacitor values of C_{12} and C_{34} were chosen by testing various values and observing the control voltage waveshape. (Their final values appear later in this chapter.) C_{12} and C_{34} must be equal or asymmetry results in the control phase voltage.

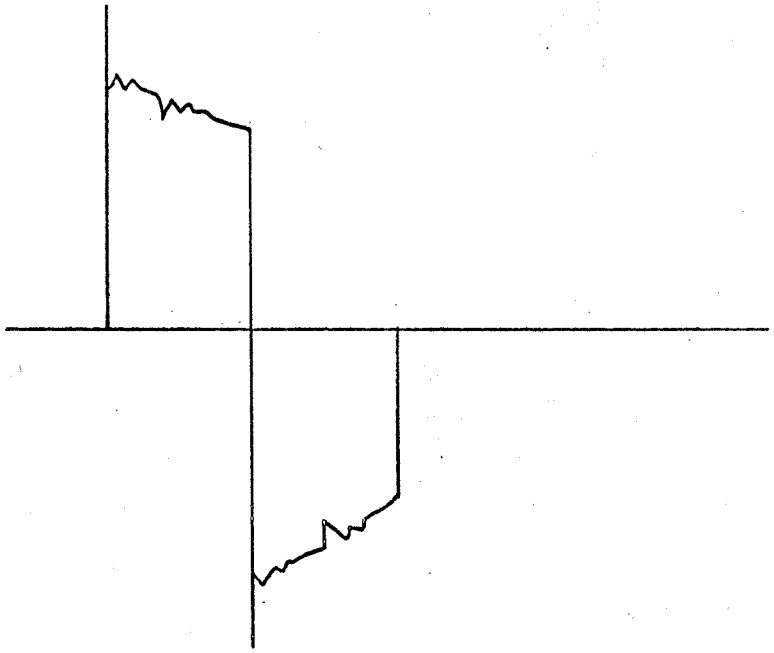

FIGURE 4 THE 400 CYCLE SUPPLY VOLTAGE OUTPUT WAVEFORM

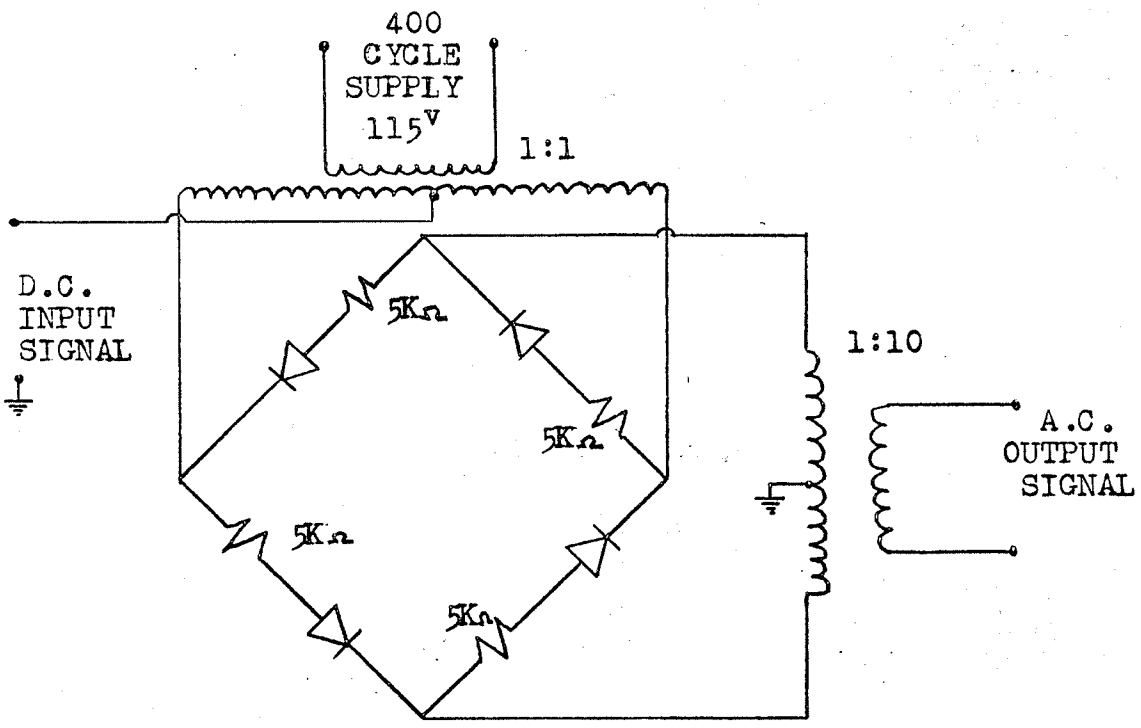

FIGURE 5 D.C. TO 400 CYCLE A.C. MODULATOR

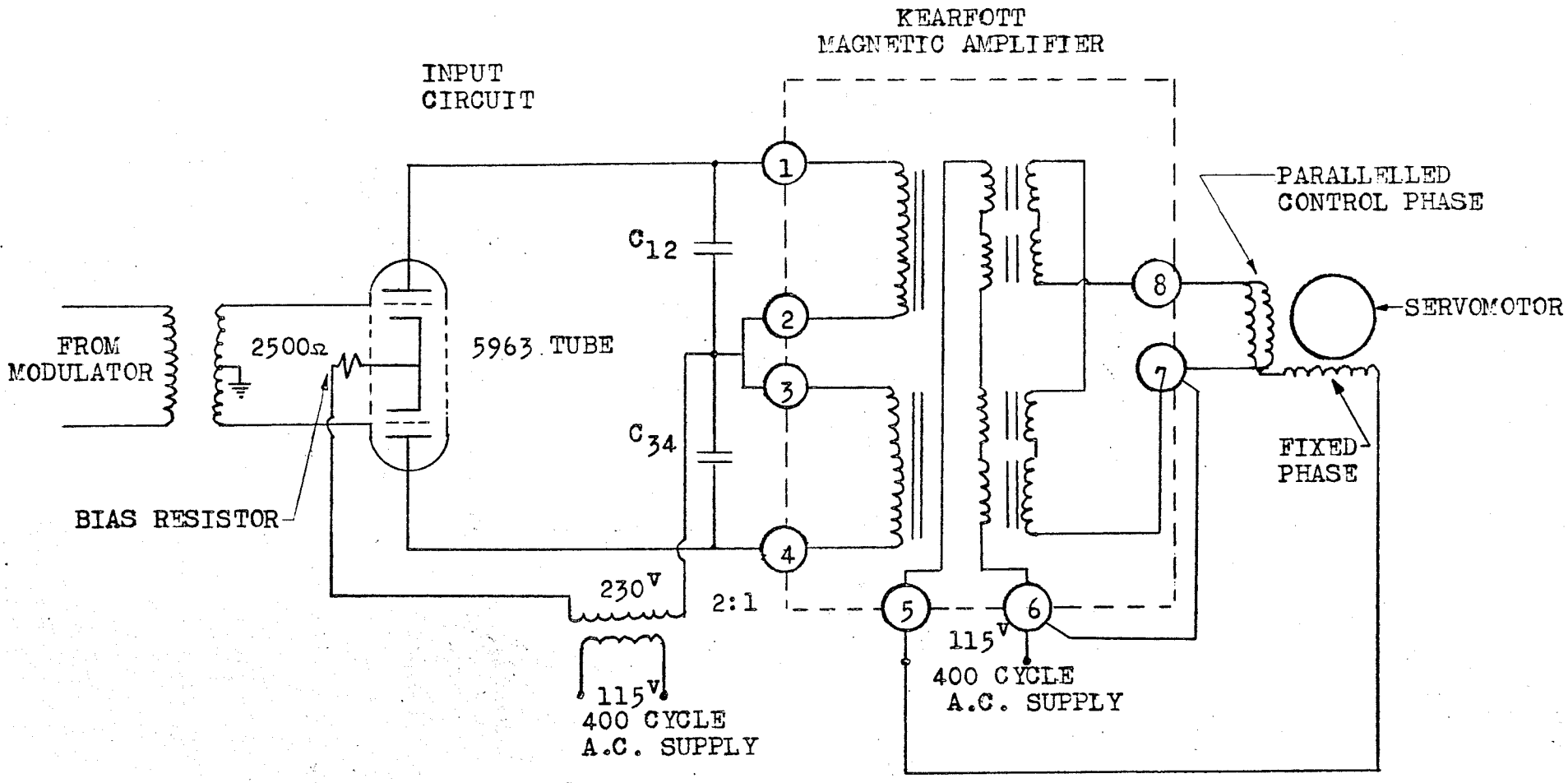

FIGURE 6 INPUT CIRCUIT, MAGNETIC AMPLIFIER, AND SERVOMOTOR

The value of the biasing resistor, about 2500 ohms, was chosen by varying its value to give a maximum control phase voltage. It may be noted here that a balanced 12AU7A may be used in place of the 5963, but will not give as good results since it does not have a specially designed long life cathode for use under on-off conditions.

The optimum capacitor value to be used in the control phase of the motor was found by recording motor torque while changing the value of the capacitor. To measure the torque, the motor was connected to a series of gears which stepped up the torque considerably and from the gears via an arm attached to the last gear which pressed on a small weigh scale. Although rather crude, this arrangement gave a resolution of about 5% in the choice of capacitor value (recorded in part 2 of this chapter).

A Lissajous Figure test was also attempted to insure that control phase and fixed phase voltages were 90° out of phase. However due to the odd waveshape of the fixed phase voltage a circle could not be obtained. As capacitance was increased toward the correct value as found in the torque test the Lissajous figure broadened and approached a square shape at the optimum value, returning to a narrower figure as this value was surpassed. The circuit and results of the Lissajous Figure test may be seen in Fig. 7.

The capacitor value could also have been determined by calculation. However due to lack of knowledge of source impedances, the quicker practical method was chosen.

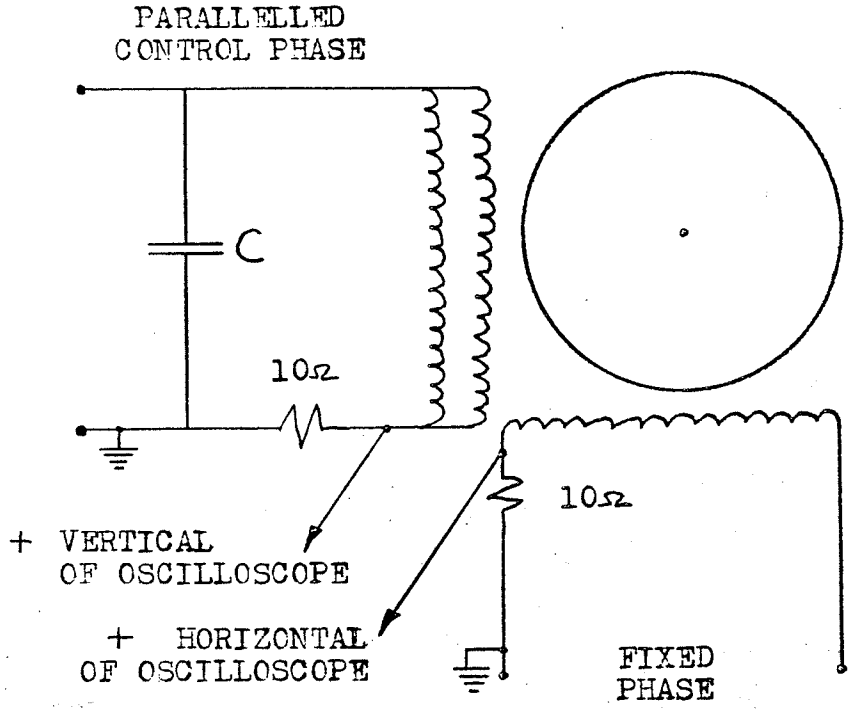

a)

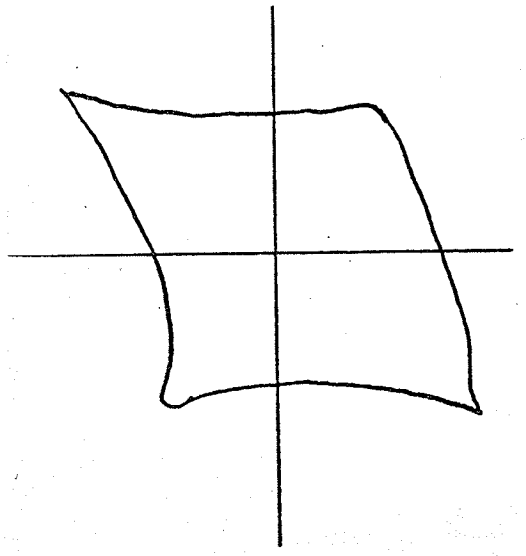

b)

FIGURE 7 a) CIRCUIT FOR LISSAJOUS FIGURES TEST
b) RESULTING FIGURE

Setting the attenuator simply involved the mechanical problem of changing rotary motion into linear motion. This was accomplished by using a linear translator and building appropriate connections. A reference potentiometer was connected to the translator such that for full travel of the attenuator, the potentiometer would make approximately a complete revolution.

A D.C. feedback system as shown in Fig. 8 was designed for temporary use so that system components could be connected together and the system could be checked in the rough. The 1500 ohm resistor was used since it was known that this was the source impedance of the VSWR meter, which was to be in the final design. Intuitively it would be expected that the smallest potentiometers available should be used since this allows maximum error current to the modulator. This is verified mathematically in Appendix B, and thus 1000 ohm potentiometers were used.

2. PIECING THE SYSTEM TOGETHER AND SOLUTION OF EXISTING PROBLEMS

The complete system was now connected together as shown in Fig. 9 and tests on its performance were carried out.

The first problem encountered was the magnitude of the control phase voltage (across terminals 7 & 8 Fig. 9). Attempts were made to increase this voltage to its required value of 150 volts r.m.s. by turning up the 400 cycle supply voltage. However this resulted in the control phase voltage waveform starting to collapse from a good sinusoidal waveform at about 300 volts peak to peak.

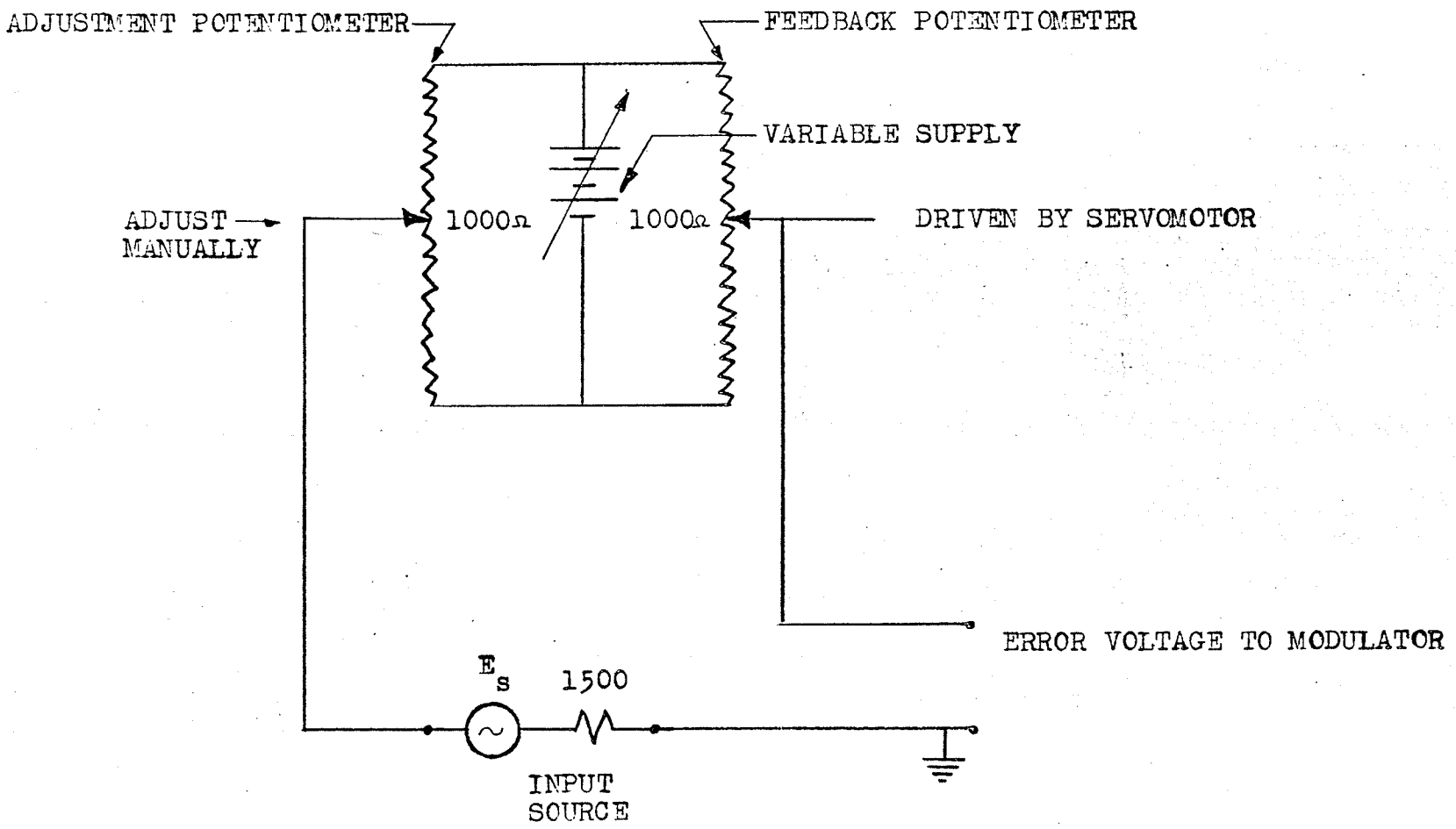

FIGURE 8 TEMPORARY D.C. FEEDBACK SYSTEM

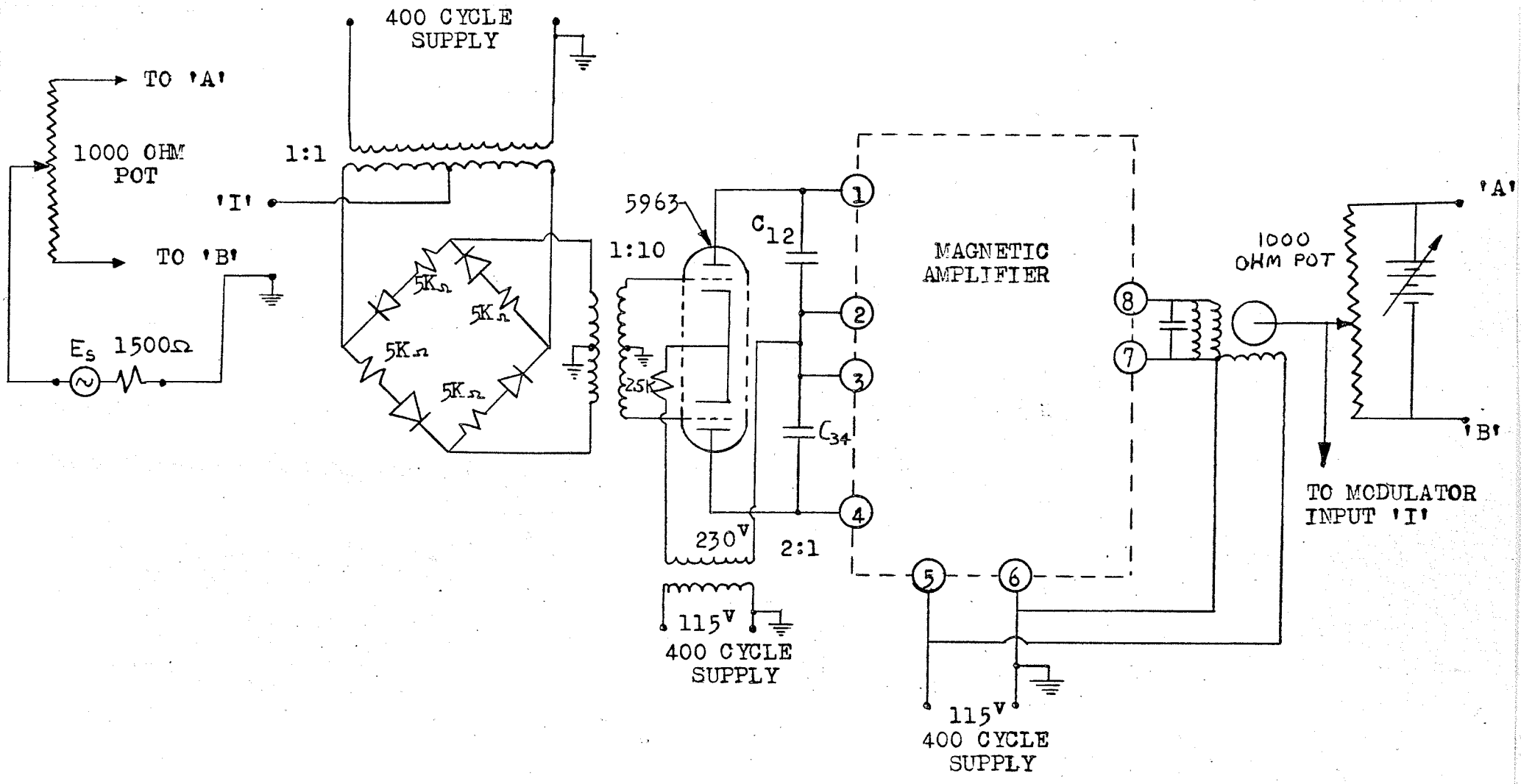

FIGURE 9 THE COMPLETE SYSTEM AS IT WAS FIRST CONNECTED

Consequently the servomotor would have to run at slight undervoltage. This seemed particularly acceptable since the non-sinsoidal waveform to the fixed phase was causing the motor to heat.

It was difficult to zero the motor since transients leaking through from the 400 cycle supply caused the motor to jitter. This was cured by the system of grounding as shown in Fig. 9.

Since the output from the VSWR meter was specified to be 0 to $\pm$ 1.5 volts D.C., the control system was now tested with this voltage as input. An oscilloscope showed that the voltage to the control phase was of a different magnitude for the same value of positive and negative input voltage. This asymmetry was traced back to the modulator. All modulator components were checked and replaced but the non-linearity still existed. The problem basically was to zero the motor with zero D.C. input (i.e. input shorted) and at the same time have the control phase voltage equal in magnitude for both positive and negative D.C. inputs, which saturated the system. This necessitated the establishing of independent control over zeroing the motor and over the magnitude of the control phase voltage.

Several biasing arrangements were tried in the circuit of the 5963 tube, but were unsuccessful. Finally it was found that a balance potentiometer placed in the modulator, as can be seen in Fig. 10, corrected the motor zeroing problem. The maximum magnitude adjustment of control phase voltage for positive and negative inputs was solved by placing variable resistors in series with diodes which were back to back in the modulator circuit as can be seen in Fig. 10. Fig. 11 gives a curve of control phase voltage versus D.C. output voltage.

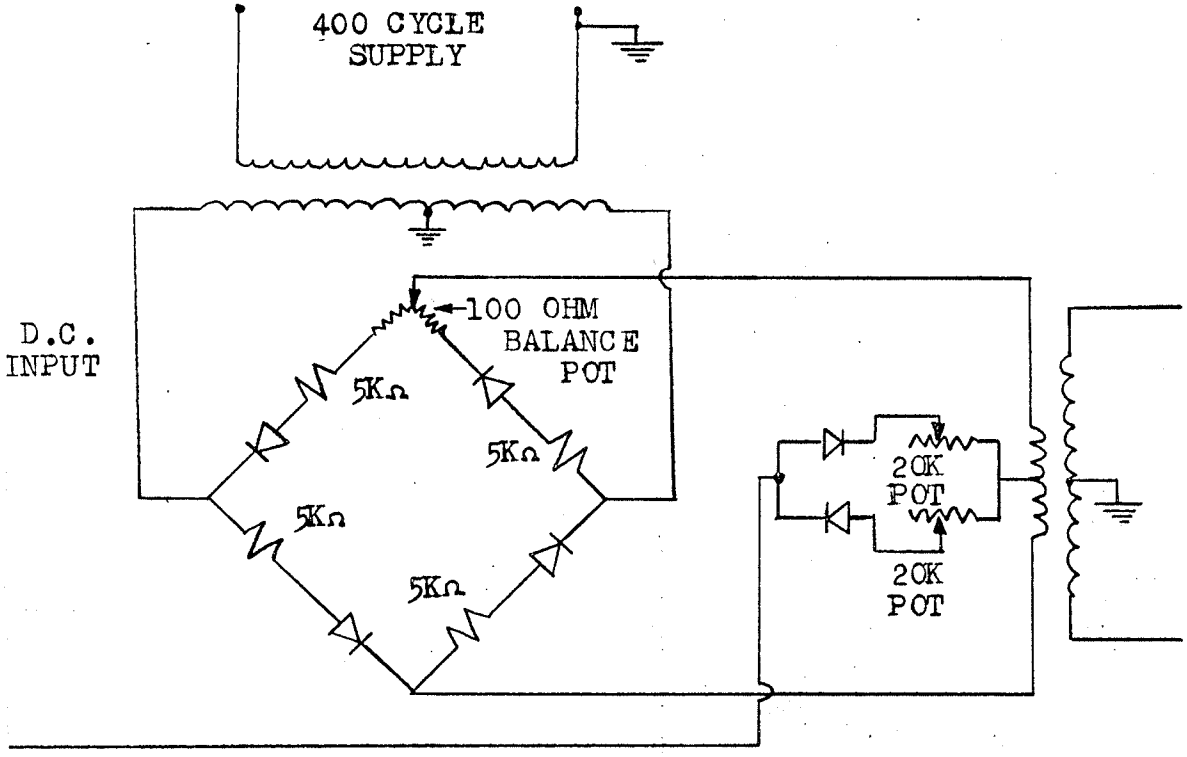

FIGURE 10 MODULATOR CIRCUIT AFTER CHANGES

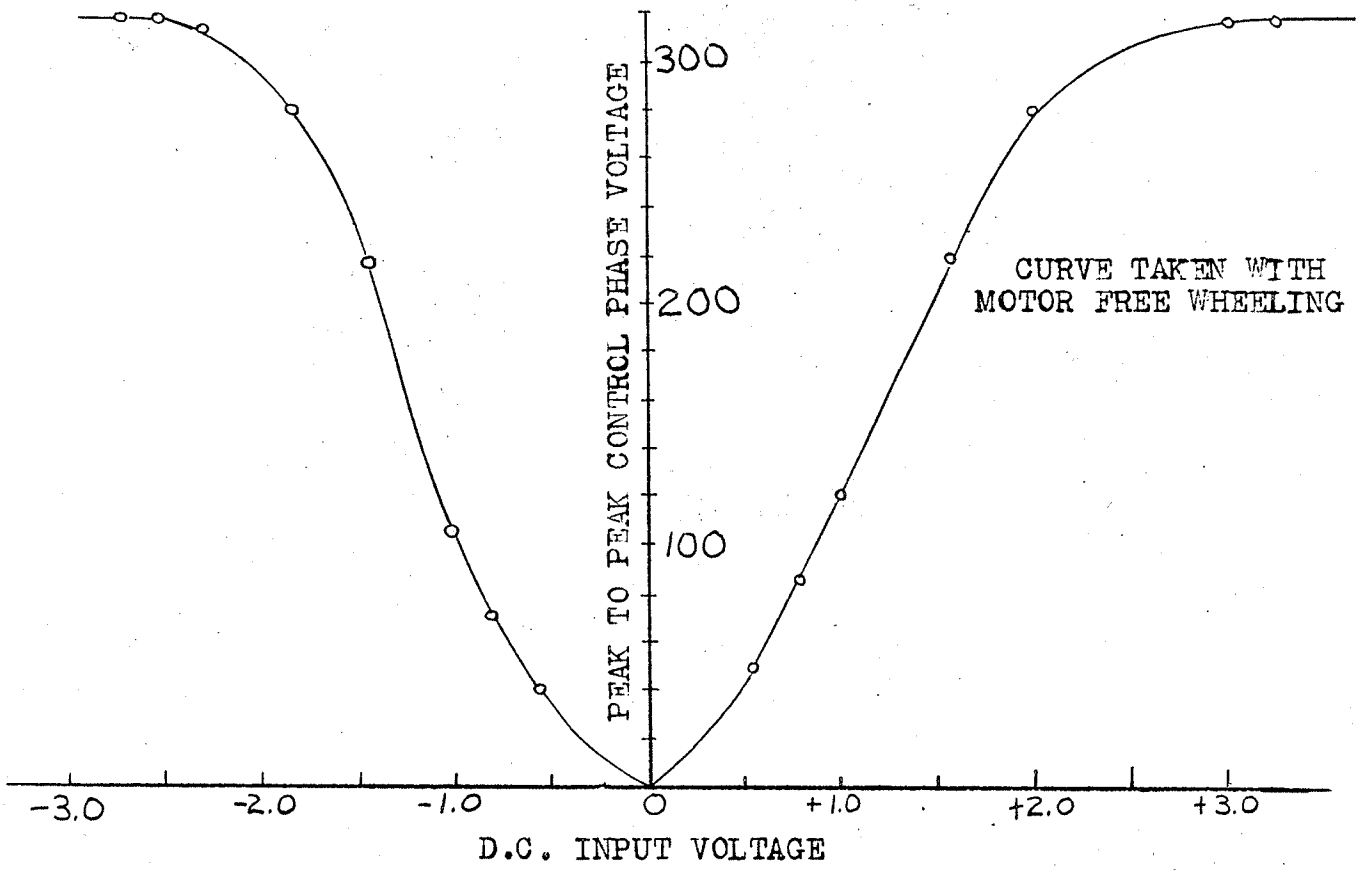

FIGURE 11 D.C. INPUT VOLTAGE VS. CONTROL PHASE VOLTAGE PEAK TO PEAK

Thus independent motor zeroing and maximum value of control phase voltage were established.

However with this new arrangement excessive noise leaked through to the control phase causing motor jitter and a new grounding system had to be instituted, as shown in Fig. 10.

It was found that with these changes, values of C_{12}, C_{34} and C had to be altered to $C_{12}= C_{34}=0.1\mu f$ and $C = 1,8\mu f$ from $C_{12}= C_{34} = .05\mu f$ and $C = 1.7\mu f$. This was again done by the same method as previously stated to obtain maximum motor torque.

The system was then completely connected together using feedback and tested with the attenuator and output and feedback pots as load. It was found to have a critical lack of gain since it was sluggish and displayed no overshoot ot step inputs.

To improve gain several amplifying arrangements were tried in the 400 cycle A.C. section between the 5963 tube and magnetic amplifier. These were unsuccessful however, and finally the Philbrick Model1 UPA-2 D.C. amplifier was found to be satisfactory when placed in front of the modulator.

When the UPA-2 was set for a gain of about 20, and with a gear ratio of 40/130 x 40/130 = 1.10.6 from motor to translator, a good response was obtained for a step input of 1.5 volts. The value 1.5 volts was used since it was expected that it would cover the complete dynamic range of input voltage. A smaller step input, if large enough to put the motor into saturation, would still give an identical overshoot.

This gear ratio was ideal since it offered a response with about 10 per cent overshoot and small steady state error. Later, after compensation testing had been completed, some backlash had developed in the linear translator to attenuator connection and after tightening the connection the resulting increase of stiffness required the gear ratio to be increased to 1/42.3.

Next a frequency response test was run in order to design a compensator for the system. The results are shown in Fig. 12 and a Nyquist plot of the results is given in Fig. 12a. For this test the D.C. amplifier was removed and the input was limited to 3.4 volts peak to peak so that the control phase voltage did not enter the saturation region. More will be said of this in Chapter 4.

Now the system was ready for adaptation to the actual microwave system. To do this the D.C. feedback loop was replaced with the attenuator acting as feedback to adjust the error signal to zero. The input was changed over to the VSWR meter output. This output, it was found, was not smooth D. C., but rather full wave rectification of 1000 cycle. This caused motor chatter and had to be filtered. An RC filter with R = 5.6K and C = 2 μf giving a cutoff of 1/RC = 89.4 radians per second placed at the output of the VSWR meter was found to be satisfactory. This filter necessitated a change in D.C. amplifier gain from 20 to 70. A reference potentiometer was placed in the input circuit. The actual control system except for compensation was now completed.

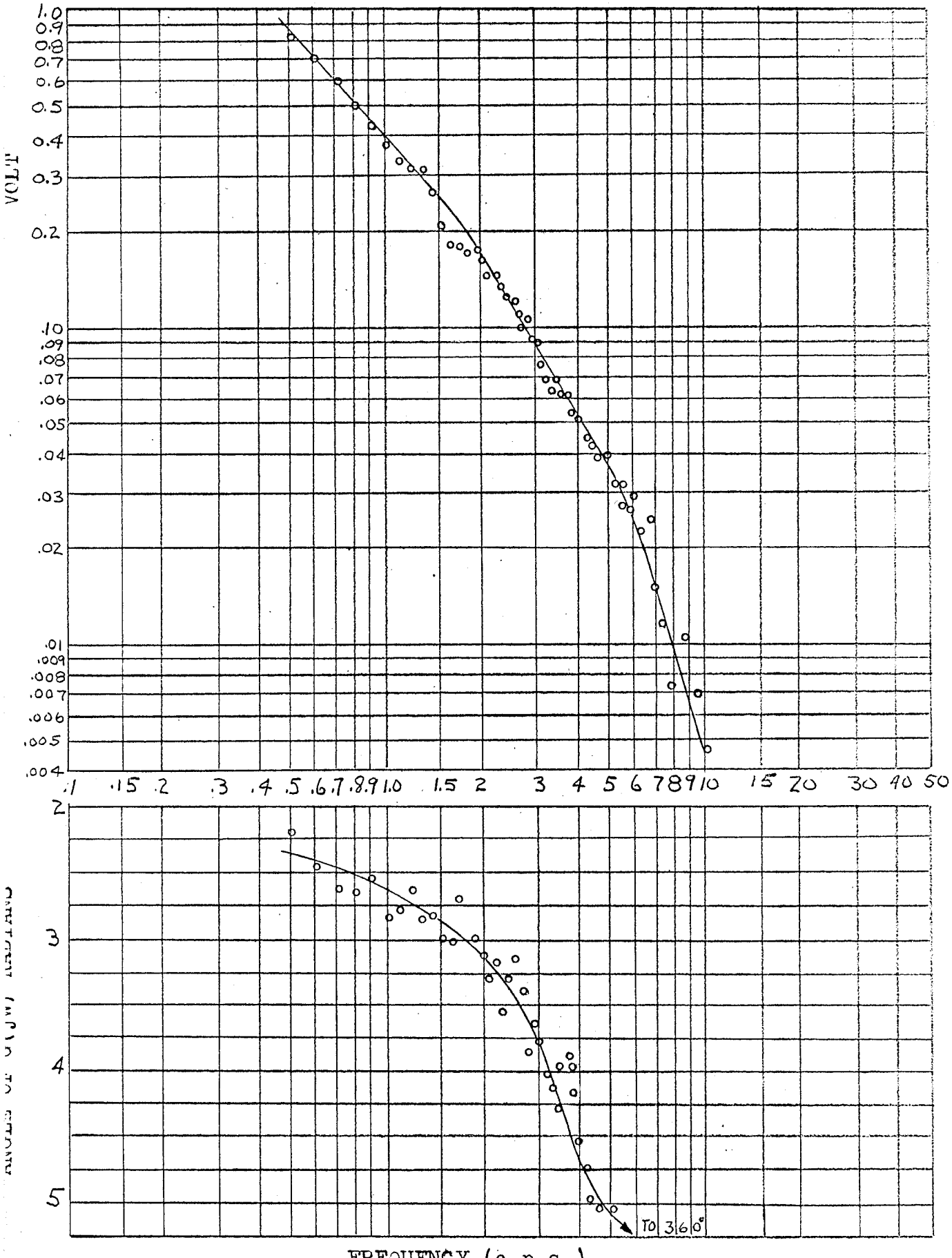

FIGURE 12 RESULTS OF FREQUENCY RESPONSE TEST

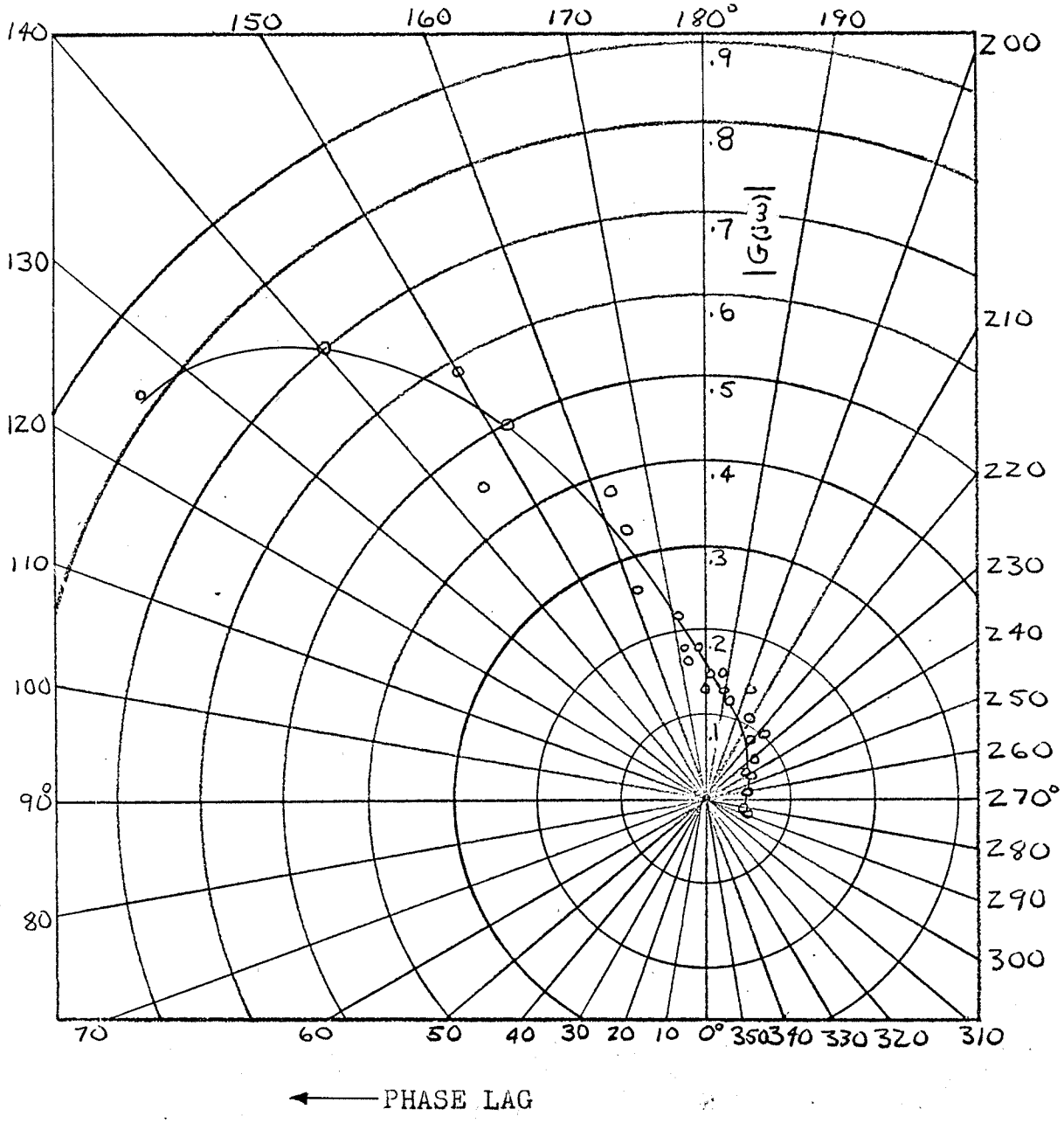

FIGURE 12a NYQUIST PLOT OF RESULTS OF FREQUENCY RESPONSE TEST

CHAPTER 4

ATTEMPTED COMPENSATION AND FINAL SYSTEM CHARACTERISTICS

This chapter begins with an outline of how the compensation problem was treated and its results, and ends with a description of the final control system characteristics.

The Bode diagram resulting from the frequency response test would seem to have a break frequency at 1.5 c.p.s. and possibly another at 6 c.p.s. These values were, however, somewhat doubtful as can be easily seen from Fig. 12, page 22. Another factor to be kept in mind was the non-linearity of the system due to saturation of the control phase voltage. This means the Bode plot, although taken without incurring saturation, cannot be accurately represented by the mathematics once saturation occurs.

Taking this information into account, a lag-lead compensator was designed with the approximate values shown in Fig. 13. These values were not attained from stringent performance specifications, but rather from the fact that it was desired to improve steady state error, and transient response, and this general compensator shape should give some improvement. If this proved to be the case the design could then be optimized. For this design the gain constant of 70 for the D.C. amplifier should remain unchanged or slightly increased, if possible, and stability should be good with little overshoot for about an 8 db step change in input. The figure 8 db arises from the fact that a larger step change in input will saturate the VSWR meter and the D.C. signal from this meter becomes erroneous

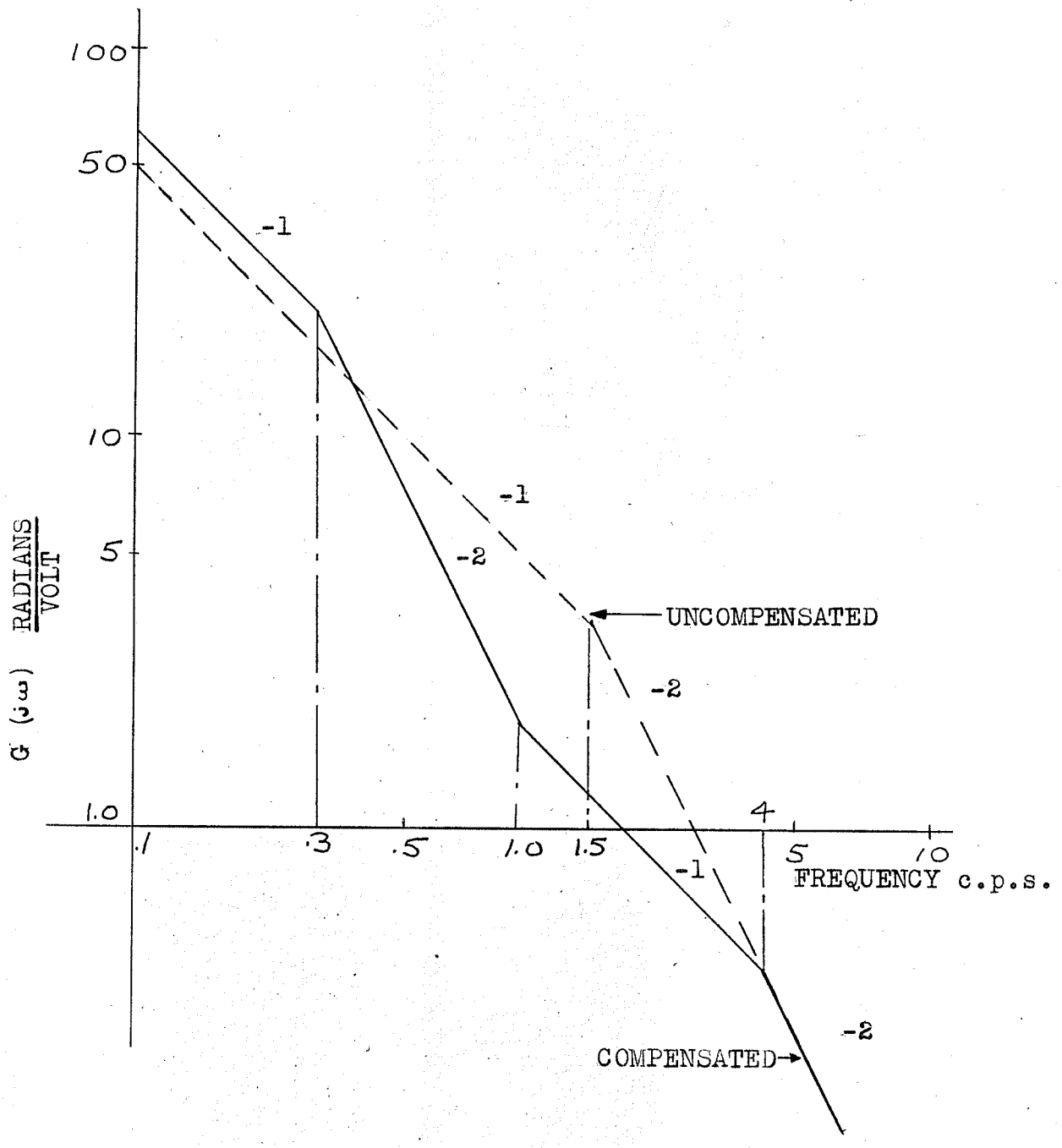

FIGURE 13 GENERAL CHARACTERISTICS OF COMPENSATED BODE PLOT

resulting in the control system not following the original change in microwave input. This point will be explained more clearly later. A precision attenuator placed in the waveguide feeding the input horn to the system would allow this step change to be made by hand.

A lag-lead network was thus fabricated and placed in front of the D.C. amplifier, but sufficient gain could not be attained with this arrangement. Every other conceivable arrangement was tried but the D. C. amplifier always overloaded. An attempt was made to build another D.C. amplifier but it failed.

A simple lag compensator was next tried and it allowed the D.C. amplifier to function properly. A large number of break frequencies were tried varying from .01 - 3 c.p.s. Almost every range between these two extremities was covered, for example .1 - .3 c.p.s. etc. It may be noted that this trial and error approach was used since it was assumed to be quicker and more conclusive than re-running a frequency test to get an exact Bode plot for a D.C. amplifier gain of 70. The mechanical attenuator connections make it difficult to take readings at low frequencies without the possibility of damaging equipment.

The method of testing was to simply feed in a step change of 8 db actuating the attenuator from its lowest limit to attenuate 8 db.

From theory a considerable improvement in steady state error with little or no change in transient response should have been the result for this type of compensation. However the best transient response, obtained with only the small improvement of two times in

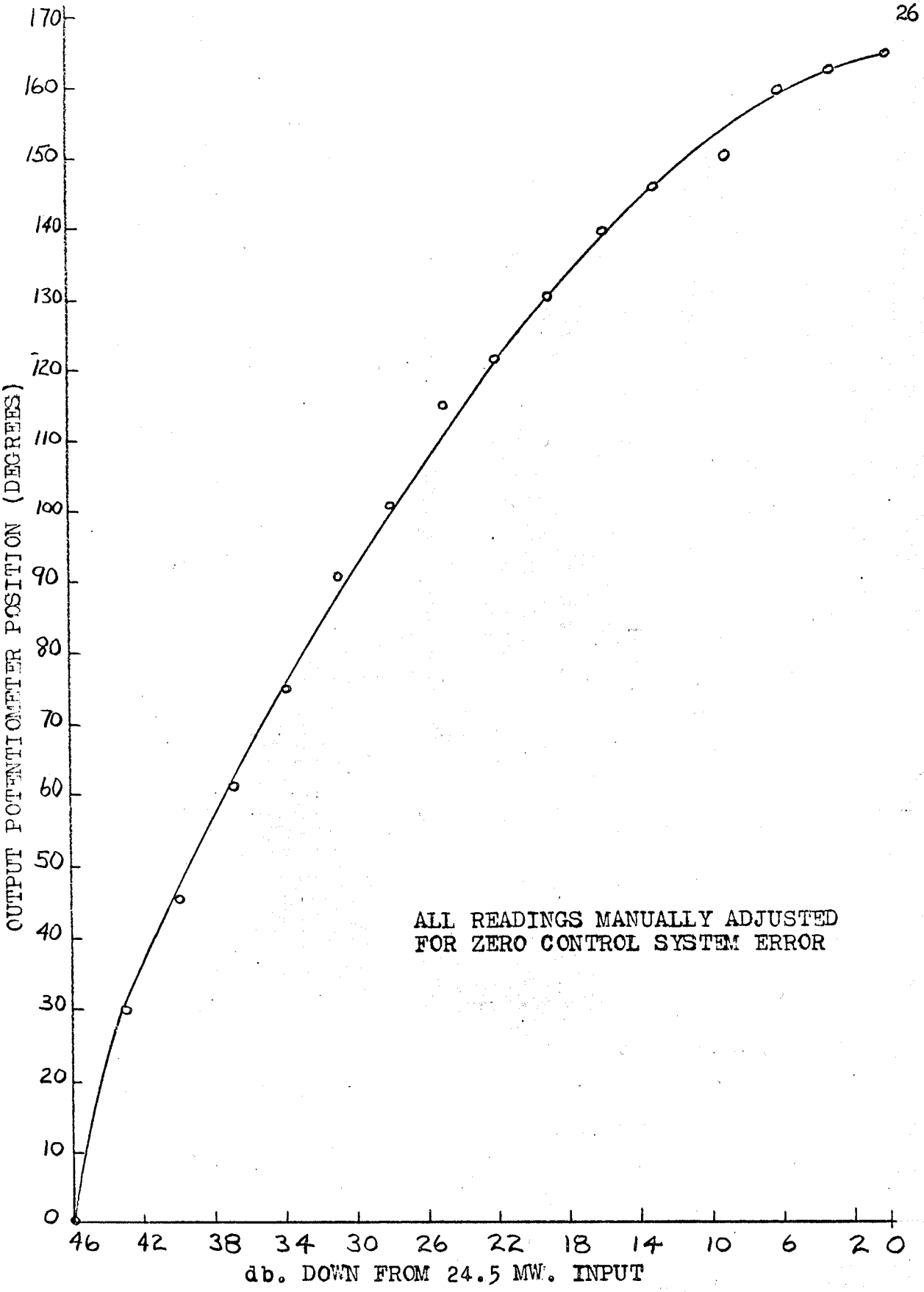

FIGURE 14 STATIC CHARACTERISTICS OF COMPLETE SYSTEM

steady state error theoretically, involved a settling time about twice as long after the first overshoot, as without compensation. Thus it could only be concluded that the control system functioned best with no compensation whatsoever.

The static characteristics of the system were next measured and found to be as shown in Fig. 14. Going from 46 db to 0 db on the abscissa of Fig. 14 corresponds to the variable attenuator going from 0 db to 46 db. Thus, for example, at 10 db down from 24.5 MW input on the abscissa the variable attenuator will be attenuating 36 db. It can be seen that about the first 16 db of attenuation, that is from 46 db to 30 db on the abscissa, is reasonably linear with output potentiometer position. After this curvature changes abruptly which means that feedback gain increases rapidly from 16 db to 46 db, or from 30 db to 0 db on the abscissa. This can be easily seen by comparing a 10° movement of the output potentiometer on the lower portion of the curve, say from 10° to 20°, which corresponds to about a 2 db change in attenuation to 10° change from, say 150° to 160°, which corresponds to about a 6 db change in attenuation.

By actual testing an approximately optimum gain curve was found over the range 0 - 40 db. The criterion of optimality employed here was that the response to an 8 db step input should have a slight overshoot, as shown in Fig. 17, Page 32. Thus 8 db step inputs were applied at regular intervals of 5 db (i.e. 0, 5, 10 etc.) from 0 - 40 db and corresponding optimum gain values were recorded. It was also found from testing that this curve could deviate considerably from the values shown in Fig. 15, and still give about the same

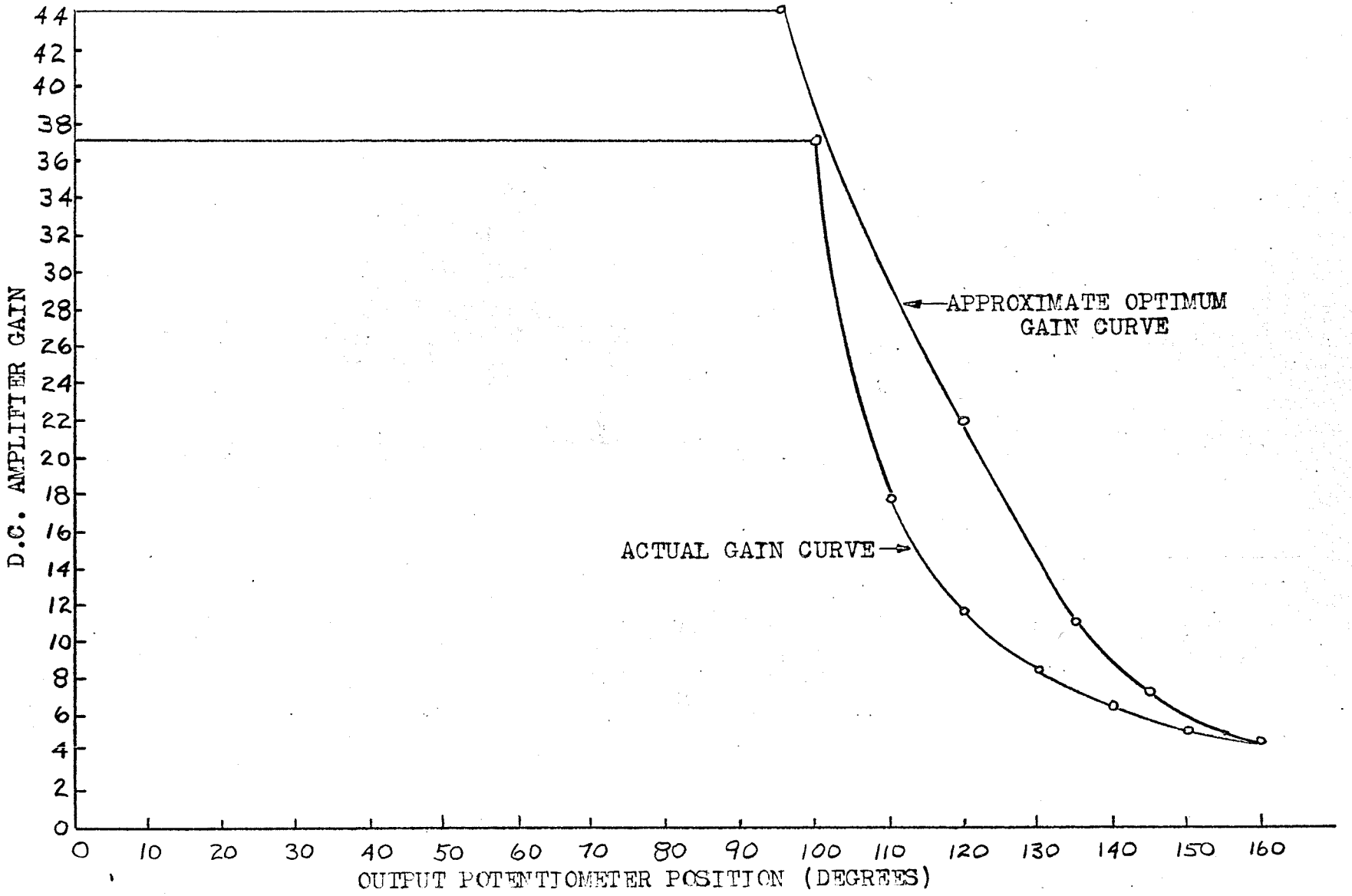

FIGURE 15 VARIABLE GAIN CURVE

results. This is the reason for the seeming discrepancy between the formerly stated D. C. amplifier gain of 70 and the present optimum gain of 44. The variable gain curve was next closely approximated by using a potentiometer connected to the output potentiometer and two resistors. Upon testing the gain was found to be too high. However, when backlash was removed from the system, hence increasing friction, the variable gain worked very well over the attenuator range. Fig. 15 shows the final gain curve employed, and Fig. 15a gives the circuit which produces this curve.

A complete circuit diagram of the system appears in Fig. 16. The dynamic characteristics of the control system may be seen in Table 1 and a sample rise time is shown in Fig. 17.

The steady state accuracy was recorded at every 4 db from 0 - 40 db. This was done by zeroing the system exactly at each interval of 4 db and changing the input very slowly until the control system began to move. The input was varied by adjusting the precision attenuator. Then the error in db could be read directly from this attenuator. It may be noted that this steady state accuracy includes the effects of friction so that it is not actually "conventional" steady state accuracy. Results of this test are shown in Table 2.

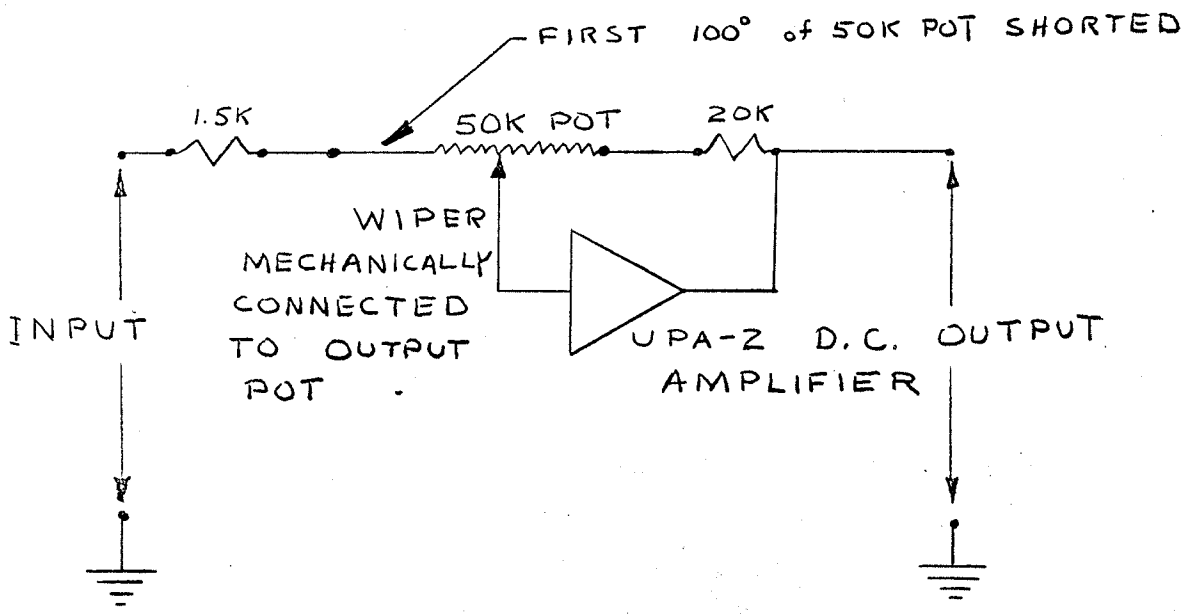

FIGURE 15a VARIABLE GAIN CIRCUIT

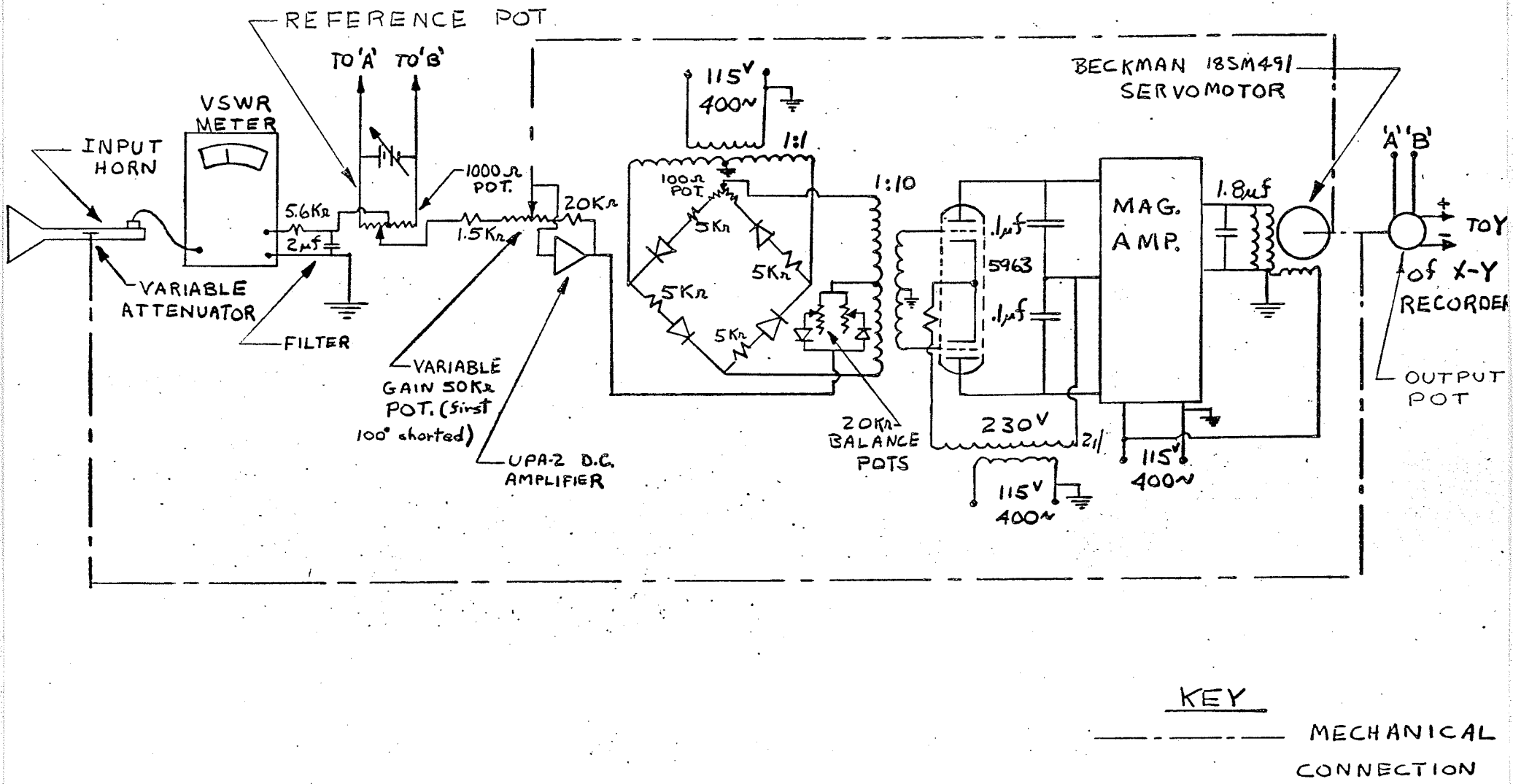

FIGURE 16 COMPLETE CIRCUIT DIAGRAM OF SYSTEM

TABLE 1

DYNAMIC CHARACTERISTICS OF THE CONTROL SYSTEM

RELATIVE STEP CHANGE IN INPUT POWER db				RISE TIME AS DEFINED IN FIGURE 16 PAGE 29 seconds
From	40	to	32	93/100
"	32	"	40	86/100
"	32	"	24	72/100
"	24	"	32	89/100
"	24	"	16	55/100
"	16	"	24	67/100
"	16	"	8	40/100
"	8	"	16	60/100
"	8	"	0	51/100
"	0	"	8	58/100

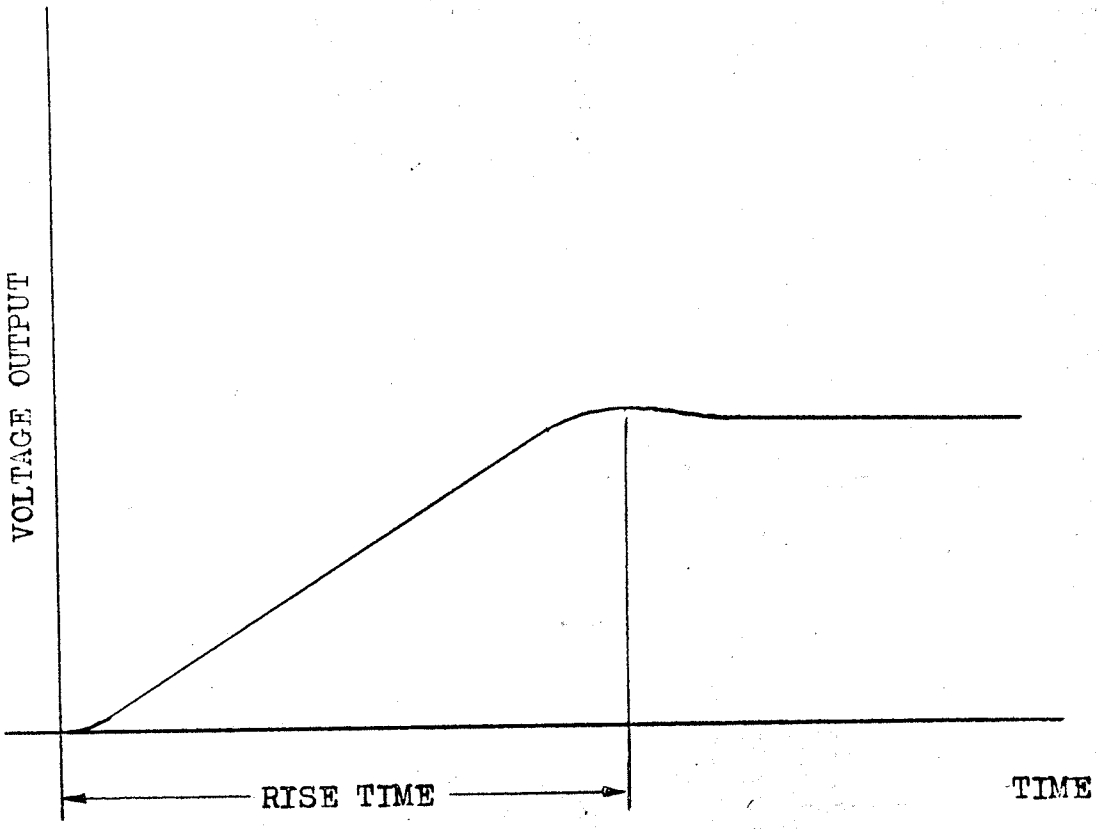

FIGURE 17 SAMPLE RESPONSE CHARACTERISTICS FOR 8 db. STEP CHANGE IN INPUT TO CONTROL SYSTEM

TABLE 2

STEADY STATE ACCURACY CHARACTERISTICS OF THE CONTROL SYSTEM

db DOWN FROM MAXIMUM INPUT POWER FOR THE TEST db	POSSIBLE db READING AS RECORDED BY CONTROL SYSTEM db
40	39.9 to 40.1
36	35.9 to 36.1
32	31.8 to 32.1
28	27.7 to 28.2
24	23.7 to 24.4
20	19.5 to 20.5
16	15.0 to 17.0
12	11.0 to 12.0
8	7.0 to 9.0
4	2.8 to 5.3
0	0 to 1.3

CHAPTER 5

EQUIPMENT LAYOUT, OPERATING INSTRUCTIONS, AND SUGGESTIONS FOR IMPROVEMENT

The physical layout of actual control equipment is in two blocks, the control chassis, and the servomechanism breadboard.

The control chassis contains the modulator, input circuit to the magnetic amplifier, and the magnetic amplifier itself. Externally it has controls for zeroing the motor by balancing the modulator and for equalizing both polarities of the control phase voltage. It also contains terminals for the 400 cycle supply input, input from the D.C. amplifier and output to both phases of the motor. All terminals and balancing controls are clearly labeled. The chassis itself must be well grounded.

The servomechanism breadboard contains the servomotor, gear train, variable attenuator and horn, the crystal, RC filter, output and reference potentiometers, and variable gain network. Leads from this breadboard to the D.C. amplifier, VSWR meter, and X-Y recorder are also clearly labeled.

The schematic in Fig. 18 supplemented by the photograph in Fig. 19, may make the physical layout of equipment and its connection clearer.

Before using the control system it is important that the modulator potentiometer and control phase balance potentiometers are properly balanced.

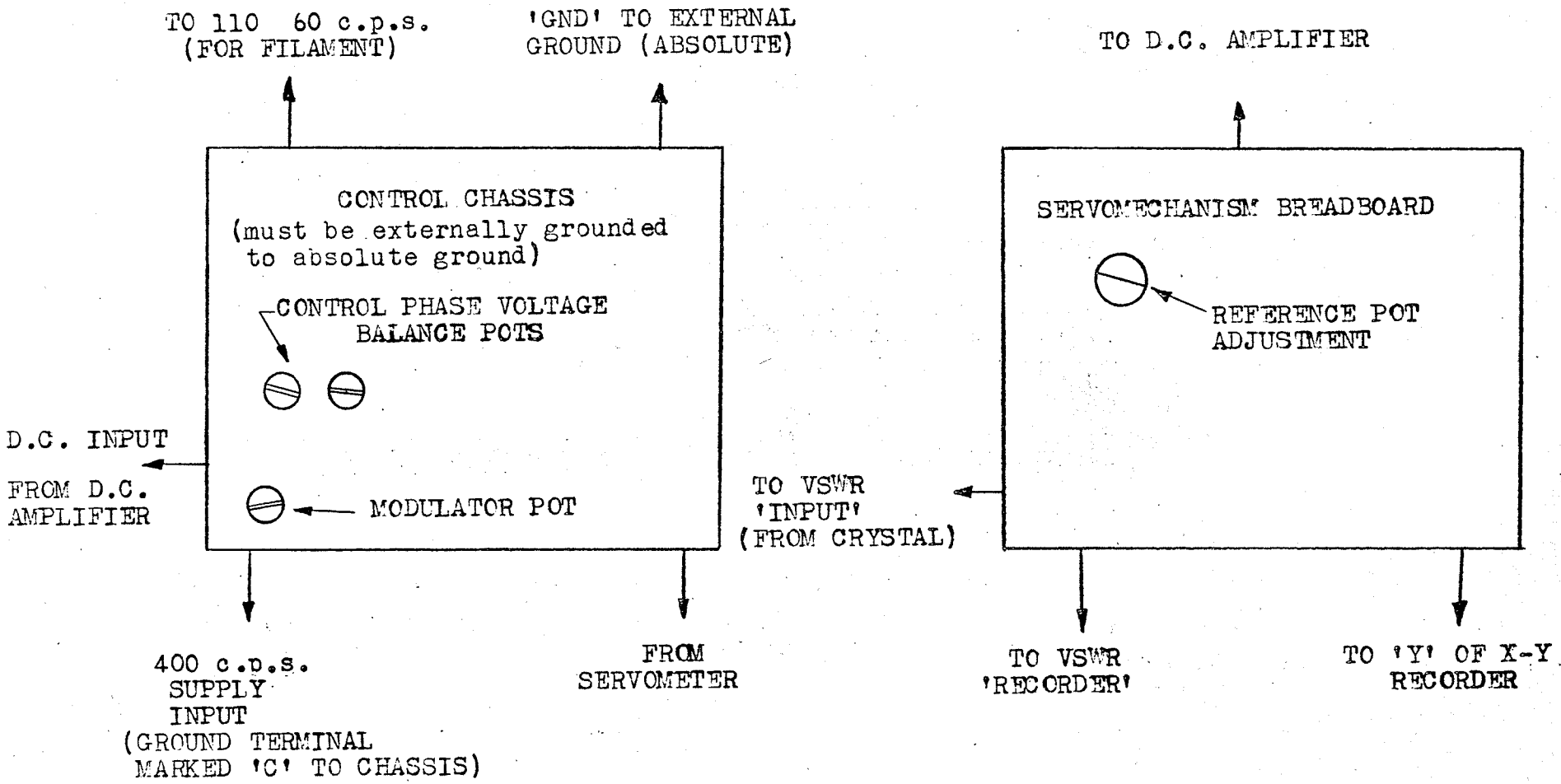

FIGURE 18 SCHEMATIC LAYOUT OF CONTROL SYSTEM

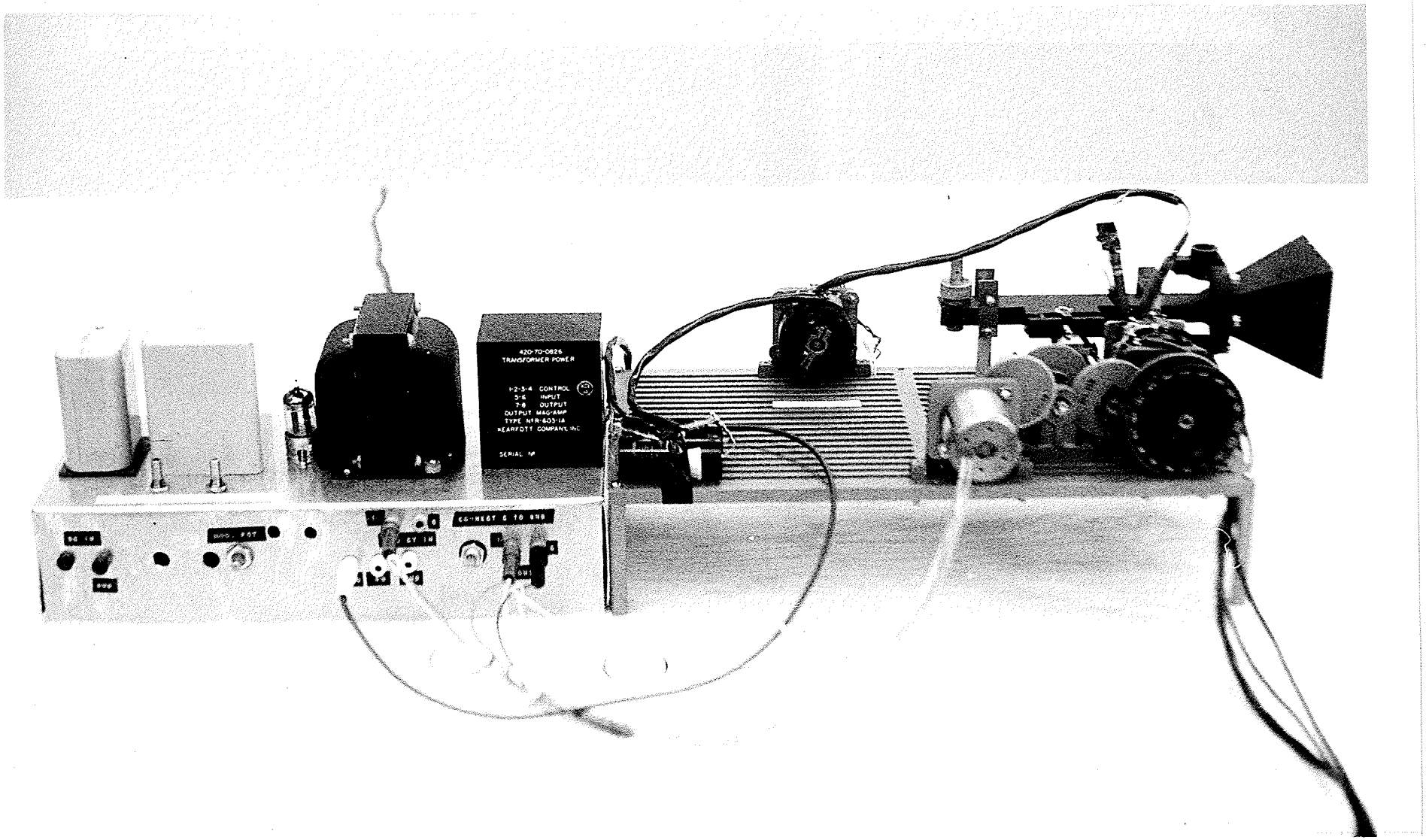

FIGURE 19 THE TWO MAIN CONTROL BLOCKS

To check this disconnect the D.C. amplifier from the control chassis being careful not to short it. Then short out the D.C. input terminal on the chassis, to ground. Next disengage the servomotor from the gears, turn on the equipment and allow it to warm up. Adjust both 20K potentiometers to zero resistance and then adjust the modulator potentiometer for motor zero. Remove the short from the input and reconnect the D. C. amplifier. By means of the reference potentiometer, saturate the control phase voltage. This will become evident when this voltage is displayed on an oscilloscope. Check both polarities and adjust the saturated values to equivalence by the appropriate 20K balance potentiometer.

A convenient value for the D.C. supply voltage feeding the reference and output potentiometers is about 5 volts for the reference potentiometer. If it is desired to have a higher value of voltage across the output potentiometer, a separate supply may be used here since a high voltage across the reference potentiometer makes the motor difficult to zero.

Preparations may now be made to take a pattern measurement. First with the motor still mechanically disengaged, and with the variable attenuator set at zero attenuation, that is, with the largest gear tight against the stop, the minimum signal in the antenna pattern to be recorded should be fed into the system. The VSWR meter may then be adjusted to 5 on the 3-10 SWR scale by means of the gain control. This value, 5, was chosen since it is approximately at the center of the VSWR meter output range and since if this meter saturates off scale an error will be incurred.

If the range switch on the VSWR meter must be set at less than 30 with gain full on for this minimum input, then crystal square law operation is exceeded and external attenuation must be used. This is however, highly unlikely. Now adjust the reference potentiometer to zero the motor. The motor may now be connected and the antenna pattern recorded. If the VSWR meter needle saturates off scale the speed of rotation of the receiving antenna under test (variable from 0 - 3 r.p.m.) must be reduced until no saturation occurs. For the test the output potentiometer will, of course, be connected to the Y input of the X - Y recorder with the X speed set in accordance with the speed of rotation of the transmitting antenna. The foregoing instructions are outlined in Table 3 for easy reference.

Some improvements in the control system could still be made. One noteworthy improvement concerns the mechanical connection which actuates the attenuator. The actual moving of the attenuator requires very little energy, but the device presently employed uses a great deal of energy. Thus a more efficient mechanical device here would improve the control system characteristics considerably.

The circuitry in the control chassis could be made more compact thus reducing pickup.

A better 400 cycle supply could also be employed. The spurious signals from the existing supply make voltage analysis difficult. If another supply is employed caution should be exercised in its ground connections to the control chassis. Reference to the circuit diagram in Fig. 16, Page 30 will be of assistance in observing this point.

TABLE 3

OUTLINE OF OPERATING INSTRUCTIONS

FOR TAKING A PATTERN MEASUREMENT

With the motor mechanically disengaged, control chassis adjustments made, and equipment warmed up, the following procedure may be employed.

1) Feed in the minimum signal, set VSWR meter to 5 on SWR scale with range switch at 30, 40, 50, or 60, and zero motor with reference potentiometer.

2) Engage motor and run antenna pattern.

3) If the VSWR meter saturates off scale, reduce the r.p.m. of transmitting antenna and re-run the pattern. Repeat until no saturation is incurred.

APPENDIX A

THE 400 CYCLE SUPPLY

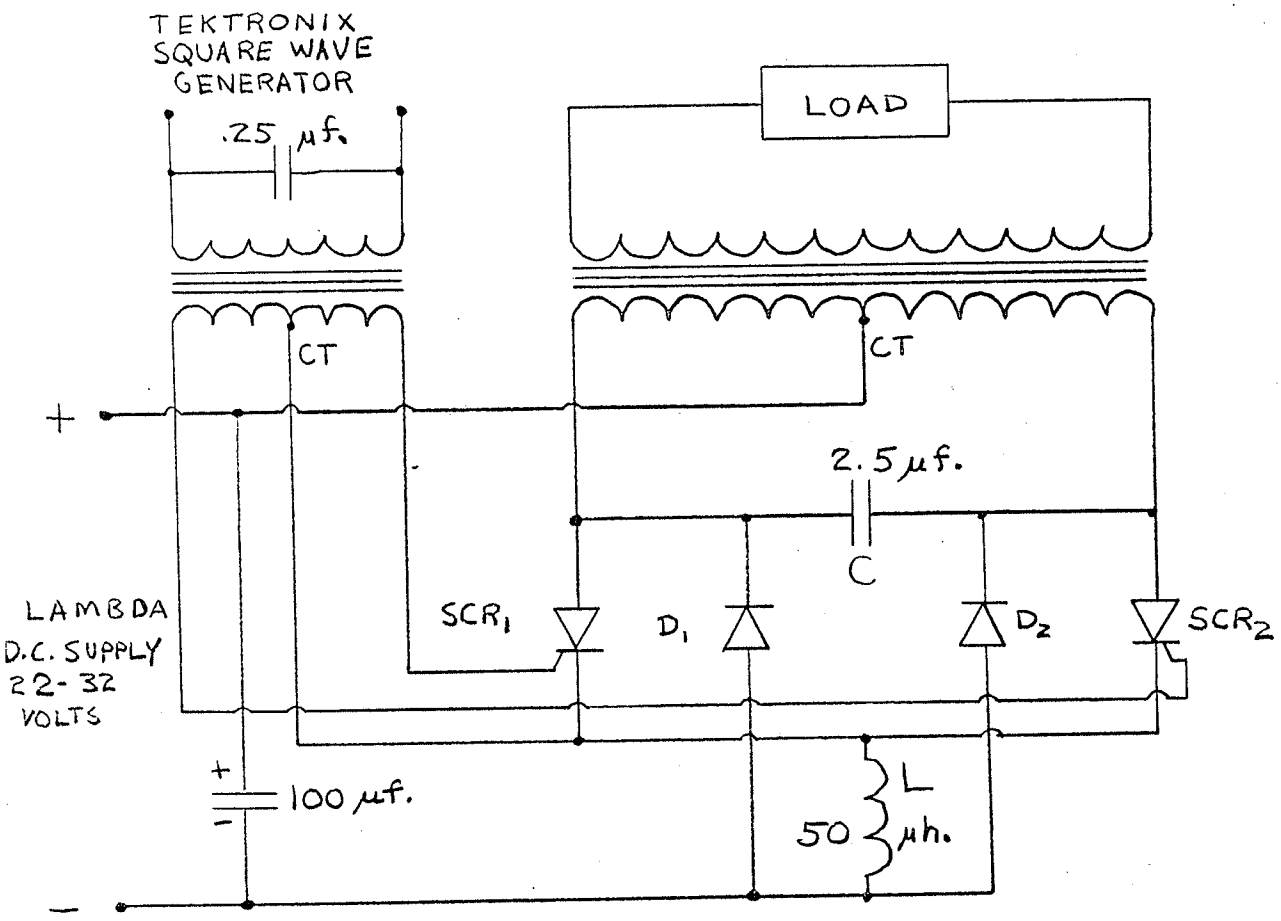

The operation of the above circuit may be briefly described as follows[2]:

"If SCR_1 is turned on by a positive gate voltage, current from the Lambda supply produced by a voltage **E** will then flow through the left hand side of the transformer. Autotransformer action produces a voltage of approximately 2E at the anode of SCR_2, and also across the 2.5 μ f capacitor. At the time a positive voltage is applied to the

gate of SCR_2 , the voltage at the gate of SCR_1 is negative, and cannot cause SCR_1 to conduct (this does not cause SCR_1 to cease conducting).

Turning on SCR_2 causes the voltage of approximately 2E to appear momentarily at the top end of the 50μh choke, reverse biasing SCR_1 , and causing it to cease conduction.

The 2.5μf capacitor and 50μh choke maintain the reverse bias across SCR_1 to recover to the blocking state. The gate of SCR_1 next goes positive, while that of SCR_2 goes negative, and the cycle is repeated.

Current is thus drawn from the D.C. supply alternately through the left and right sides of the transformer primary, causing an A.C. voltage (essentially a square wave) to appear at the transformer secondary.

The feedback diodes D_1 and D_2, though not necessary to the operation of the inverter, contribute greatly to its performance. Feedback occurs at the switching or commutating interval. Thus the method of commutation is entirely different from that of most parallel inverters, although the circuits are superficially similar. The diodes, and the capacitor accross the D.C. supply are the only differences.

The discharge of capacitor C through L is oscillatory. When the anode of SCR_2 goes below ground, diode D_2 conducts. This will occur at the end of the commutation interval of SCR_1 (i.e. after SCR_1 has ceased conduction). The conduction of diode D_2 causes the remaining energy stored in L (which is no longer necessary for commutation since SCR_1 has ceased conduction) to be fed back to the anode of SCR_2.

Thus a small amount of the discharge of C through L is used to turn off the SCR's, while the balance of the energy is fed back and dissipated in the forward direction of the feedback diode, the conducting SCR, and the winding resistance of L.

This oscillatory discharge, then does not appear at the load, and the wave form is essentially a square wave, except for a spike and a small amount of ringing during the commutating interval.

Another advantage offered by the diodes is that the circuit is enabled to operate under a range of loads varying from rated load to open circuit, depending upon the dissipation capabilities of the SCR's, the diodes, and the inductor L, as the load condition of open circuit is approached."

APPENDIX B

CALCULATION OF OPTIMUM POTENTIOMETER SIZE TO MAXIMIZE INPUT CURRENT TO MODULATOR

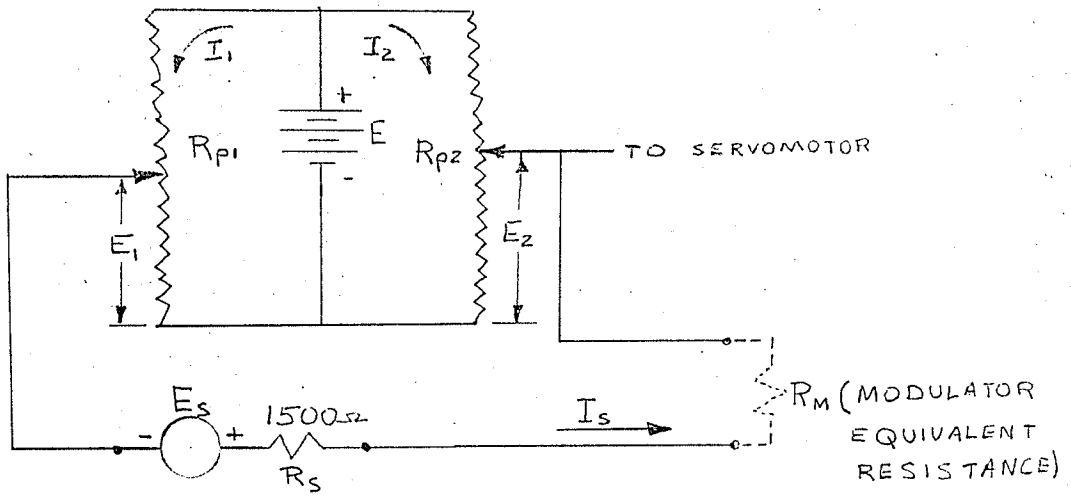

Let R_{p1} = total resistance of potentiometer 1

R_{p2} = total resistance of potentiometer 2

f_1 = fraction of resistance of potentiometer 1 across which E_1 is seen

f_2 = fraction of resistance of potentiometer 2 across which E_2 is seen

Now the following equations may be written:

$$E = 0 + I_2 R_{p2} + I_s f_2 R_{p2}$$

$$E = I_1 R_{p1} + 0 + (-I_s f_1 R_{p1})$$

$$E_s = -I_1 f_1 R_{p1} + I_2 f_2 R_{p2} +$$

$$I_s (R_M + R_s + f_2 R_{p2} + f_1 R_{p1})$$

Solving for I_s :

$$I_s = \frac{E_s + E(f_1 - f_2)}{R_M + R_s + R_{p1}(f_1 - f_1^2) + R_{p2}(f_2 - f_2^2)}$$

Thus it is obvious that R_{p1} and R_{p2} should be as small as practically possible.

BIBLIOGRAPHY

1. Weinschel Engineering, Application Note #5, 1960

2. Anderson, R.A., Cork, K., Parallel Inverter Employing Silicon Controlled Rectifiers (Undergradute Thesis, Dept. of Electrical Engineering, University of Manitoba E636, 1963)

3. Law, J., Schmitz, N.L., Transient Response Characteristics of an A.C. Servomotor Excited Nonsinusoidally and Through Nonlinear Source Impedances (P. A. & S. June 1964, Vol. 83 No. 6)

4. Ahrendt, W. R., Savant, C.J., Servomechanism Practice, McGraw-Hill Book Company, Inc., New York, Toronto, London, 1961

5. Bower, J.L., Schultheiss, P.M., Introduction to the Design of Servomechanisms, John Wiley and Sons Inc., New York, London, 1958